Contents
Previous Section

Physical Properties of Clastic Reservoir Rocks in the Uinta, Wind River, and Anadarko Basins, As Determined by Mercury-Injection Porosimetry

By C.W. Keighin

GEOLOGIC CONTROLS OF DEEP NATURAL GAS RESOURCES IN THE UNITED STATES

U.S. GEOLOGICAL SURVEY BULLETIN 2146–G

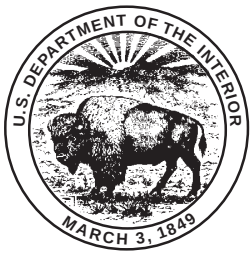

UNITED STATES GOVERNMENT PRINTING OFFICE, WASHINGTON : 1997

CONTENTS

FIGURES

TABLES

Physical Properties of Clastic Reservoir Rocks in the Uinta, Wind River, and Anadarko Basins, As Determined by Mercury-Injection Porosimetry

By C.W. Keighin

ABSTRACT

Pores, and pore throats, in clastic rocks from three sedimentary basins were studied petrographically and by mercury-injection porosimetry. Samples represent a variety of sedimentary facies, as well as a wide range of depths, and diverse diagenetic histories. Although pore throats may be limiting features in controlling fluid flow in low-permeability sandstones, very few data are available with which to document the effect of confining stress typical of reservoir conditions on capillary pressure or pore-throat size. Understanding the nature of pore throats, and their relationship to facies distribution and to diagenesis, aids in understanding mechanisms of fluid flow in clastic rocks. This information is valuable for calculating hydrocarbon recovery from potential reservoir rocks.

INTRODUCTION

Although studies documenting the effects of confining stress on porosity and permeability in clastic rocks have been made, almost no data are available with which to document the effects of confining stress on pore-throat size distribution when this size distribution has been determined by mercury-injection capillary pressure studies. Mercury-injection porosimetry may be especially useful for understanding reservoir behavior in deep sedimentary basins.

In this paper, I document the usefulness of mercury-injection porosimetry in identifying reservoir quality for deep reservoir rocks using data from several basins. Nineteen rock samples from the Uinta, Wind River, and Anadarko basins were examined using standard petrographic techniques and mercury-injection porosimetry to understand the pore-throat structure and overall petrophysical characteristics of reservoir rocks from the deeper parts of the basins. Samples were chosen to represent a wide variety of depositional environments, and petrological suites were selected from both reservoir and nonreservoir rock facies. Individual samples may have been taken from producing or nonproducing horizons from known reservoir rocks. Samples were taken from different depth intervals, each of which may reflect a different diagenetic history. The three basins from which samples were collected all contribute significant quantities of oil or natural gas to the Nation's energy resource base.

SANDSTONE PETROGRAPHY

Geographic location and stratigraphic position for each sample are given in table 1. Sample depth and a summary of modal analyses and porosity-permeability values are listed in table 2. Photomicrographs of selected samples are shown in figure 1. Because the samples are from widely separated geographic locations and from different depositional environments, their petrologic properties differ significantly. The small number of samples examined in this study limits extrapolation of the results to other basins, although similar rocks might be expected to have similar properties.

The samples vary primarily in the relative abundance of quartz, feldspar, and rock fragments (table 2); carbonate cement is locally abundant. The relative abundance of rock fragments may have a significant effect on macro- and micro-porosity and permeability. Pore size in any sample is initially related to grain size of the original sediment and thus to depositional environment. Pore size and, especially, pore-throat size may be significantly modified by physical compaction or by precipitation of mineral cements. Compression of labile rock fragments reduces intergranular porosity and creates intergranular pseudomatrix; both reduce effective permeability (McBride and others, 1991). Partial dissolution of rock fragments commonly creates microporosity; micropores introduce micro-pore-throats that restrict fluid migration.

The two samples from the Shell-Christenson well in the Uinta Basin of Utah are fine grained and quartz rich. Porosity is low in both samples but for different reasons. The sample from 11,852 ft (3,612 m) depth shows evidence of compaction, but porosity loss is due primarily to the

Table 1. Location and geologic formation for samples examined in this study.

Sample no.	Depth (feet)	Well	County	Location	Formation
		Uinta Basin, Utah			
Ch 1–35	11,852	Shell-Christenson 1–35–A5	Duchesne	Sec. 33, T.1 S, R. 5 W.	Green River.
Ch 1–35	11,932	Shell-Christenson 1–35–A5	Duchesne	Sec. 33, T.1 S, R. 5 W.	Green River.
		Anadarko, Basin, Oklahoma			
OK–1	18,076	Kerr-McGee No. 1 Tentanque	Cado	Sec. 35, T.5 N., R. 10 W.	Springer.
OK–2	16,078	Texaco No. 1 Carr	Cado	Sec. 36, T.5 N., R. 11 W.	Springer.
OK–3	11,960	Humble No. 1 Patterson	Grady	Sec. 23, T.5 N., R. 6 W.	Springer.
OK–4	12,072	Humble No. 1 Patterson	Grady	Sec. 23, T.5 N., R. 6 W.	Springer.
OK–5	16,626	Chevron 1 Berta B Lay	Grady	Sec. 8, T.3 N., R. 7 W.	Springer.
OK–6	10,161	Edwin Cox 1 Miller	Canadian	Sec. 26, T.14 N., R. 10 W.	Morrow.
OK–7	7,096	King Stevenson 1 Anderson	Woodward	Sec. 26, T.25 N., R. 20 W.	Morrow.
OK–8	7,197.5	King Stevenson 1 Anderson	Woodward	Sec. 26, T.25 N., R. 20 W.	Morrow.
OK–9	10,378	Odessa Nat. Gas 1 Milstead	Woodward	Sec. 33, T.20 N., R. 21 W.	Morrow.
		Wind River Basin, Wyoming			
WY–8	12,097.5	Monsanto 1–35 Dolis	Fremont	Sec. 35, T.39 N., R. 91 W.	Lance.
WY–10	12,111	Monsanto 1–35 Dolis	Fremont	Sec. 35, T.39 N., R. 91 W.	Lance.
WY–20	12,709.4	Monsanto 1–35 Dolis	Fremont	Sec. 35, T.39 N., R. 91 W.	Lance.
WY–21	13,483	Monsanto 1–35 Dolis	Fremont	Sec. 35, T.39 N., R. 91 W.	Lance.
WY–25	13,517.3	Monsanto 1–35 Dolis	Fremont	Sec. 35, T.39 N., R. 91 W.	Lance.
WY–27	13,527	Monsanto 1–35 Dolis	Fremont	Sec. 35, T.39 N., R. 91 W.	Lance.
WY–31	13,602.5	Monsanto 1–35 Dolis	Fremont	Sec. 35, T.39 N., R. 91 W.	Lance.
WY–35	13,631	Monsanto 1–35 Dolis	Fremont	Sec. 35, T.39 N., R. 91 W.	Lance.

presence of approximately 19 percent (by volume) carbonate cement. The sample from 11,932 ft (3,636 m) depth contains approximately 4 percent carbonate cement but is more compacted than the first sample.

Samples from the Anadarko Basin of Oklahoma (OK–1 through OK–9; fig. 1*A*, *B*, *D*) are from different wells, formations, and depths. They exhibit a large variation of porosity and permeability. There is no obvious relationship between grain size and porosity or between depth and porosity, even in the same well. Reduced porosity is most commonly related to increased cementation and sometimes to compaction of labile rock fragments or to poor sorting. Detailed petrologic data for additional samples from the Anadarko Basin are given in Keighin and Flores (1989).

Samples from the Wind River Basin of Wyoming (WY–8 through WY–35; fig. 1*C*) are typically coarser grained and contain more rock fragments than samples from the other basins. The Wind River subset is too small, however, to determine if grain size and (or) the presence of rock fragments affect the distribution of porosity or permeability. Most porosity probably is due to dissolution of rock fragments or other detrital grains. Porosity loss is due primarily to compaction; the volume of porosity-reducing carbonate cement is usually less than 5 percent.

MERCURY-INJECTION POROSIMETRY

Petrophysical characteristics of rocks influence the ability of petroleum reservoirs to produce, and an understanding of these characteristics can help to maximize production. An analytical technique useful for determining distribution of pore-throat sizes, and thus understanding the structures of pore systems in the reservoir, is capillary pressure analysis. Pore systems consist of pores and smaller channels (pore throats) connecting the pores. Pore throats, in conjunction with pore-system geometry and topology, control the movement of fluids between pores. Through the use of capillary-pressure curves derived from mercury-injection porosimetry, it is possible to calculate pore-throat size and distribution.

Mercury-injection porosimetry is based on measurement of volume distribution of pore throats; the method depends on forcing mercury into small voids, pore throats, within the rock. Pore throats control access to larger voids (pores) because greater pressures are required to force mercury, or other nonwetting fluids, into smaller spaces (see Purcell, 1949). Thus, pore throats are bottlenecks in the system, and it is necessary to exceed their critical capillary pressure in order to inject mercury into pores. By injecting mercury at incrementally higher pressures, and allowing time for equilibration between pressure increments, mercury is injected into increasingly smaller pores. It is then possible to calculate the size distribution of pore throats, to determine how pore-throat size is affected by increasing confining stress to approximate reservoir conditions, and to determine how permeability is affected by reduction in pore-throat size.

The samples in table 2 show a large range of porosity and permeability values, although porosity is typically below 8 percent and Klinkenberg permeability below 0.1 mD. Klinkenberg (1941) showed that, especially in low-permeability media, permeability to a gas is a function of the mean

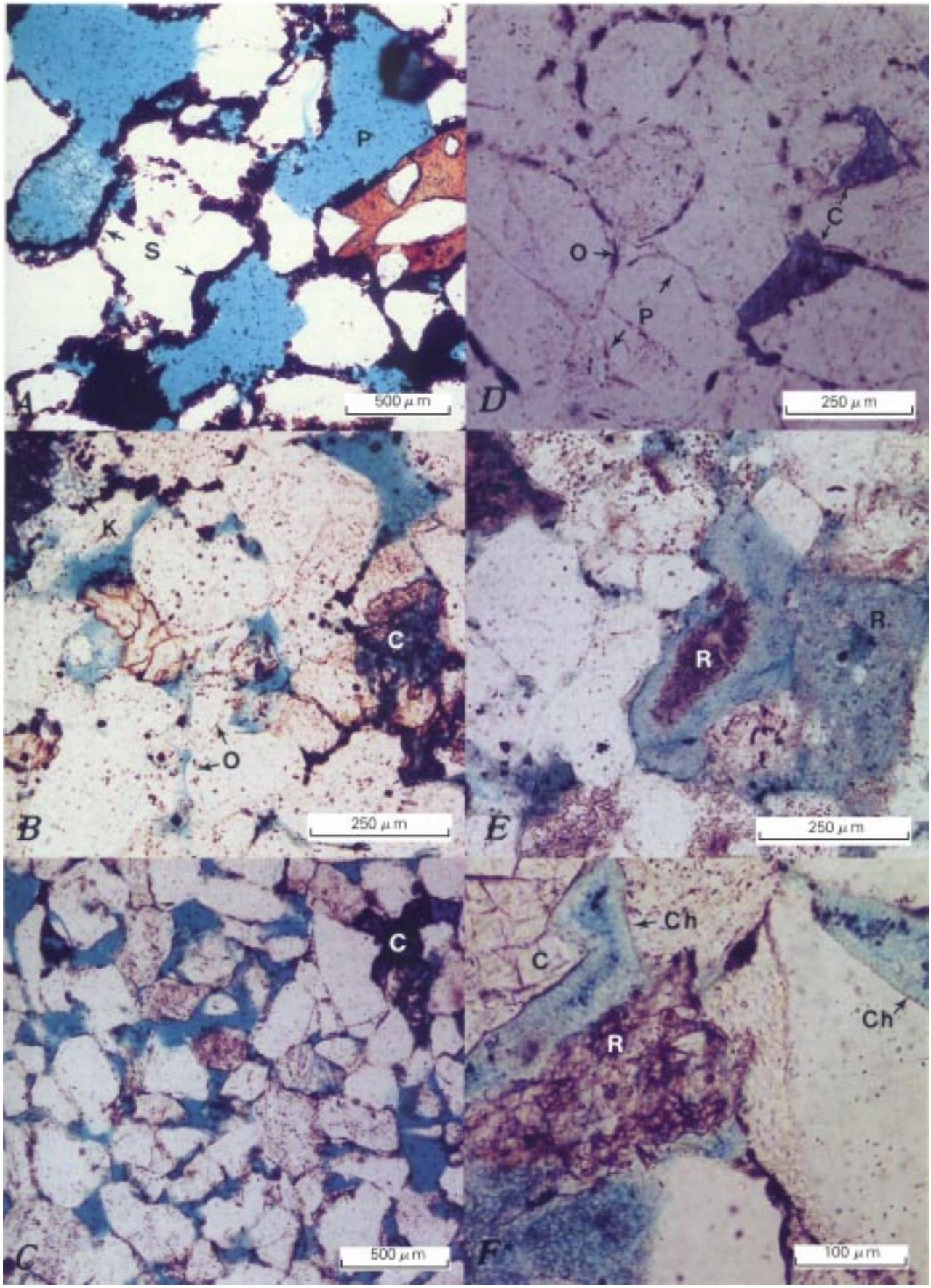
P
S
500 μm
A
O
C
P
250 μm
D
K
C
O
250 μm
B
R
R
250 μm
E
C
500 μm
C
Ch
C
Ch
R
100 μm
F

Figure 1 (previous page). Photomicrographs of thin sections prepared from plugs on which porosity-permeability and mercury-injection determinations were made. Location of samples is given in table 1, and porosity, permeability, and modal analysis results are given in table 2. All photographs taken in plane-polarized light. *A*, Sample OK–7. Depth, 7,096 ft (2,163 m); helium porosity, 16 percent; in situ permeability, 330 mD. Good porosity and permeability are created by large, open pores (P); pores are generally clay free but are typically lined by wheat-grain siderite (S). Neither porosity nor permeability has been reduced by compaction or chemical cementation in this sample. *B*, Sample OK–8. Depth, 7,198 ft (2,194 m); helium porosity, 14.1 percent; in situ permeability, 47.7 mD. Sample is poorly sorted but clean (few rock fragments); pores are relatively clean and open, although some are filled with kaolinite (K). Authigenic quartz overgrowths (O) and carbonate cement (C) are present, but neither porosity nor permeability has been significantly reduced by chemical cementation. *C*, Sample OK–3. Depth, 11,960 ft (3,645 m); helium porosity, 14.3 percent; in situ permeability, 86.6 mD. Sandstone is moderately sorted, fine grained, and relatively clean; pores are typically open and clay-free, although iron-bearing carbonate cement (C) is sometimes present. *D*, Sample OK–1. Depth 18,076 ft (5,510 m); helium porosity, 2.1 percent; in situ permeability, 0.0010 mD. Sandstone is well sorted and clean, but porosity and permeability have been significantly reduced by compaction, quartz overgrowths (O) (silica cementation), and pore-filling carbonate (C). Intergranular pores (P) are present but are typically very thin (<5 μm). *E*, Sample WY–8. Depth, 12,097.5 ft (3,687 m); helium porosity, 6.9 percent; in situ permeability, 0.0022 mD. Moderately sorted medium-grained sandstone contains both compacted and partially dissolved rock fragments (R); some porosity is microporosity due to partial dissolution of rock fragments; few pores are clean (free from clays or authigenic cements). Authigenic cements include silica overgrowths and intergranular carbonates. *F*, Sample WY–35. Depth, 13,631 ft (4,155 m); helium porosity, 7 percent; in situ permeability, 0.0024 mD. Medium-grained, moderately sorted sandstone is rich in rock fragments. Most pores are lined with authigenic chlorite (Ch), and many are filled with other authigenic clays. Porosity has also been reduced by precipitation of intergranular carbonate (C).

free path of the gas molecules. When gas flows through capillaries having diameters small enough to be comparable to the mean free path of the gas, as is typically the case in low-permeability media, discrepancies appear between gas and liquid permeabilities in the porous media. Klinkenberg introduced the concept of "slip" and the following equation to correct apparent gas permeability, *Kg*, of a gas flowing at a mean pore pressure, *P*, to the true permeability of the porous medium, K_∞ (see also Sampath and Keighin, 1982):

$$Kg = K_\infty(1+b/\overline{P})$$

DATA ANALYSIS

Crossplots of in situ Klinkenberg permeability versus in situ helium porosity and in situ Klinkenberg permeability versus routine air permeability for samples in this study are shown in figure 2. They indicate a generally close correlation between porosity and permeability. As expected, porosity and permeability in general decrease with depth, but depth is not the only factor to consider in the decrease of either porosity or permeability.

Schmoker and Gautier (1988) considered that porosity-reducing diagenetic reactions in the subsurface are dependent on time-temperature exposure of the formation and, further, that depth may or may not be a good measure of thermal exposure. In addition, the decrease in porosity with depth may not be uniform (Atkins and McBride, 1992, fig. 9). Examination of thin sections indicates that, although compaction due to increasing depth of burial may be a factor, the degree of compaction is greatly influenced by lithology, especially the presence and quantity of labile rock fragments (Dutton and Diggs, 1992). Cementation, either by silica or by carbonate minerals, reduces both porosity and permeability, as well as significantly modifies pore structure.

This study is particularly aimed at describing pore structure and, necessarily, determining how these structures are generated and modified. It would be especially useful in both exploration and production to be able to accurately predict porosity and the role of mechanisms responsible for modifying porosity and pore structure. Pore throats are an important aspect of overall pore structure. In part because of their small size, they are more sensitive to diagenetic modifications including physical compaction and chemical change (dissolution or precipitation of newly formed minerals). Research to date has not completely answered these questions (Harrison, 1989; Surdam and others, 1989; Bloch, 1991; Bachu and Underschultz, 1992).

Examination of the porosity and permeability data in table 2 reveals a wide variation in measured values; the data also show wide variations in the effects of confining stress on permeability. Relationships between capillary pressure and wetting-phase saturation (that is, air) and pore-size distribution for a range of porosity and permeability values are shown in figure 3 (see also McCreesh and others, 1991). The samples illustrated in figure 3*A* and *B* are among the most porous of the samples investigated and, in thin section, have the largest visible pores. Plots of pore-size frequency versus pore entry-throat diameter reveal, however, that pore throats in these samples are most commonly in the 10-μm range, significantly smaller than the pores visible in thin section. The plots also show that pore throats are constricted by increased confining stress, although not as dramatically as in samples that have lower initial porosity and permeability and smaller measured pore throats. Data plotted in figures 3*C* and *D* indicate that, for samples more typically fitting the "tight" sand designation, pore throats are more typically in the <0.1-μm size range and that these already small pores are further reduced by confining stress. Thus, even though pores visible in thin section may be relatively large, all pores must be accessed through pore throats, which are smaller,

Table 2. Sample depth, and summary of modal analyses and measured porosity and permeability for samples examined in this study.

[Sample location information is given in table 1. Modal analyses are normalized to 100 percent: Q, quartz; F, feldspar; R, lithic fragments; leaders (--) indicate not present. Properties are defined at bottom of table. Helium porosity is in situ value. Permeability values are corrected for Klinkenberg effect. ND indicates not determined]

Sample	Depth	Modal analysis (volume percent)			Properties			Porosity (percent)		Permeabilityx		In situ permeability/ ambient permeability
No.	(feet, meters)	Q	F	R	Size	Sort	Angularity	Helium	Modal	Ambient	Insitu	(percent)
Uinta Basin, Utah												
Ch 1–35	11,852 (3,612)	91.3	2.5	6.2	165	0.7	3.5	2.2	3	0.0065	0.0004	6.15
Ch 1–35	11,932 (3,637)	93.1	3.1	3.8	193	0.8	2.1	4.0	7.6	0.0165	0.0018	10.9
Anadarko Basin, Oklahoma												
OK–1	18,076 (5,510)	100	-.-	-.-	207	0.4	3.5	2.0	0.8	0.0050	0.0010	20.
OK–2	16,078 (4,901)	98.1	0.8	1.1	148	0.4	2.9	4.9	8.5	0.0729	0.0078	10.69
OK–3	11,960 (3,645)	99.6	0.4	-.-	210	0.9	2.0	13.3	24	95.466	89.6	93.39
OK–4	12,072 (3,680)	100	-.-	-.-	156	0.4	2.0	4.3	6	0.0477	0.0026	5.45
OK–5	16,626 (5,068)	99.5	0.5	-.-	140	1.0	2.5	8.8	10.8	0.5185	0.1975	38.09
OK–6	10,161 (3,097)	98.7	0.9	0.4	166	0.5	3.6	ND	15.4	ND	ND	
OK–7	7,096 (2,163)	91.4	1.0	7.6	321	0.4	3.8	14.	25	343.75	330.20	96.06
OK–8	7,197 (2,194)	99.6	0.4	-.-	209	1.7	3.8	12.8	22	50.75	47.65	93.89
OK–9	10,378 (3,163)	98.7	0.65	0.65	101	1.5	0.6	9.6	4.8	0.0078	0.0032	41.03
Wind River Basin, Wyoming												
WY–8	12,097 (3,687)	85.5	2.0	12.5	317	0.7	1.5	6.5	12.2	0.0157	0.0022	14.01
WY–10	12,111 (3,691)	85.2	0.5	14.3	162	0.5	1.5	8.2	9.5	0.0077	0.0017	22.07
WY–20	12,709 (3,874)	75.8	2.4	21.8	255	0.8	2	5.5	6.1	0.0106	0.0012	10.85
WY–21	13,483 (4,110)	60.4	3.9	35.7	330	1.0	1.8	5.9	5.7	0.0133	0.0010	7.52
WY–25	13,517 (4,120)	69.7	4.3	26.	226	1.2	1.2	3.7	4.1	0.0012	0.0001	8.33
WY–27	13,527 (4,123)	77.8	3.9	18.3	317	0.8	1.5	5.2	3.3	0.0052	0.0005	9.62
WY–31	13,602 (4,146)	80	10.9	18.3	397	0.5	2.1	4.7	4.9	0.0051	0.0011	21.57
WY–35	13,631 (4,155)	62.1	15.9	22	272	0.5	2.2	6.7	7.2	0.0065	0.0024	36.92

Properties

Grain size		Sorting		Angularity	
Size (μm)	Wentworth size	Visual estimate	Degree of sorting	Class interval	Grade term
550–250	Medium sand	0–0.35	Very well sorted	2.0–3.0	Subangular
250–125	Fine sand	0.35–0.5	Well sorted	3.0–4.0	Subrounded
125–62.5	Very fine sand	0.5–1.0	Moderately sorted	4.0–5.0	Rounded
		1.0–2.0	Poorly sorted		

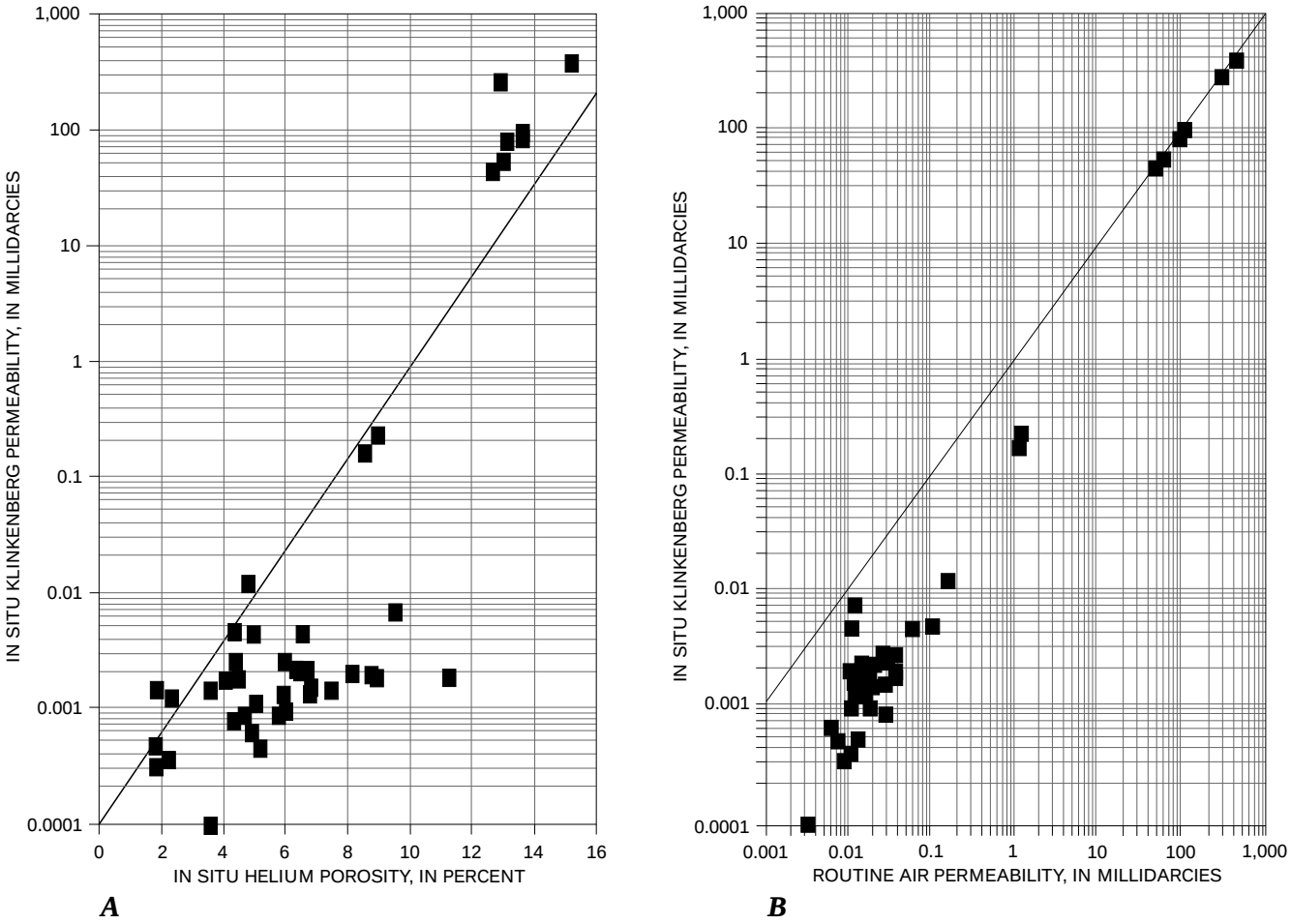

Figure 2. Cross plots of in situ Klinkenberg permeability versus *A*, in situ helium porosity and *B*, routine air permeability for samples from core in the Anadarko, Uinta, and Wind River basins.

Figure 3 (following pages). Plots illustrating capillary pressure versus wetting phase (that is, air) saturation and pore size distribution for samples under ambient (squares) and in situ (triangles) stress conditions. Location of samples is given in table 1, and porosity, permeability, and modal analysis results are given in table 2. Values of porosity and permeability given following are in situ values. *A*, Sample OK–8. Porosity, 12.8 percent; permeability, 47.65 mD; depth 7,197.5 ft (2,194 m). Shape of the capillary pressure versus saturation curve indicates that mercury entered pores at relatively low pressure and that saturation was essentially complete at approximately 7,000 psia. Although the larger pores visible in figure 1*B* are approximately 50 by 100 µm, measured pore-size distribution shows that the majority of pore throats are smaller than approximately 15 µm. *B*, Sample OK–3. Porosity, 13.3 percent; permeability, 89.6 mD; depth 11,960 ft (3,645 m). Measured porosity and visible pores in figure 1*C* suggest that properties of sample OK–3 are very similar to those of sample OK–8. The capillary pressure versus saturation curve indicates that more pore throats are being constricted by application of confining stress. The pore-size distribution curves reveal a slightly higher proportion of larger pores (although still in the 20 µm size range) in this sample as compared with sample OK–8; pore throats under confining stress are typically smaller than 15 µm. *C*, Sample WY–21. Porosity, 5.9 percent; permeability, 0.0010 mD; depth 13,483 ft (4,109 m). Capillary pressure versus saturation curves show that mercury saturation of pore space is not accomplished, even at 10,000 psia, and that entry into pores is significantly restricted with increasing confining stress. Pore-size distribution curves reveal that unconfined pore throats are typically smaller than approximately 1 µm; when under confining stress, pore throats are reduced significantly in size and are typically less than 0.05 µm. *D*, Sample OK–1. Porosity, 2.0 percent; permeability, 0.0010 mD; depth 18,076 ft (5,509 m). The physical appearance of the sample (fig. 1*D*) suggests very low porosity and permeability due, at least in part, to compaction and cementation by carbonate and silica overgrows. Examination of the thin section illustrated in figure 1*D* suggests that the "thin-film" intergranular pores may be 1–2 µm across. Pore size distribution curves show, however, that pore throats are most commonly <0.2 µm (unconfined) to 0.04–0.1 µm (confined) across.

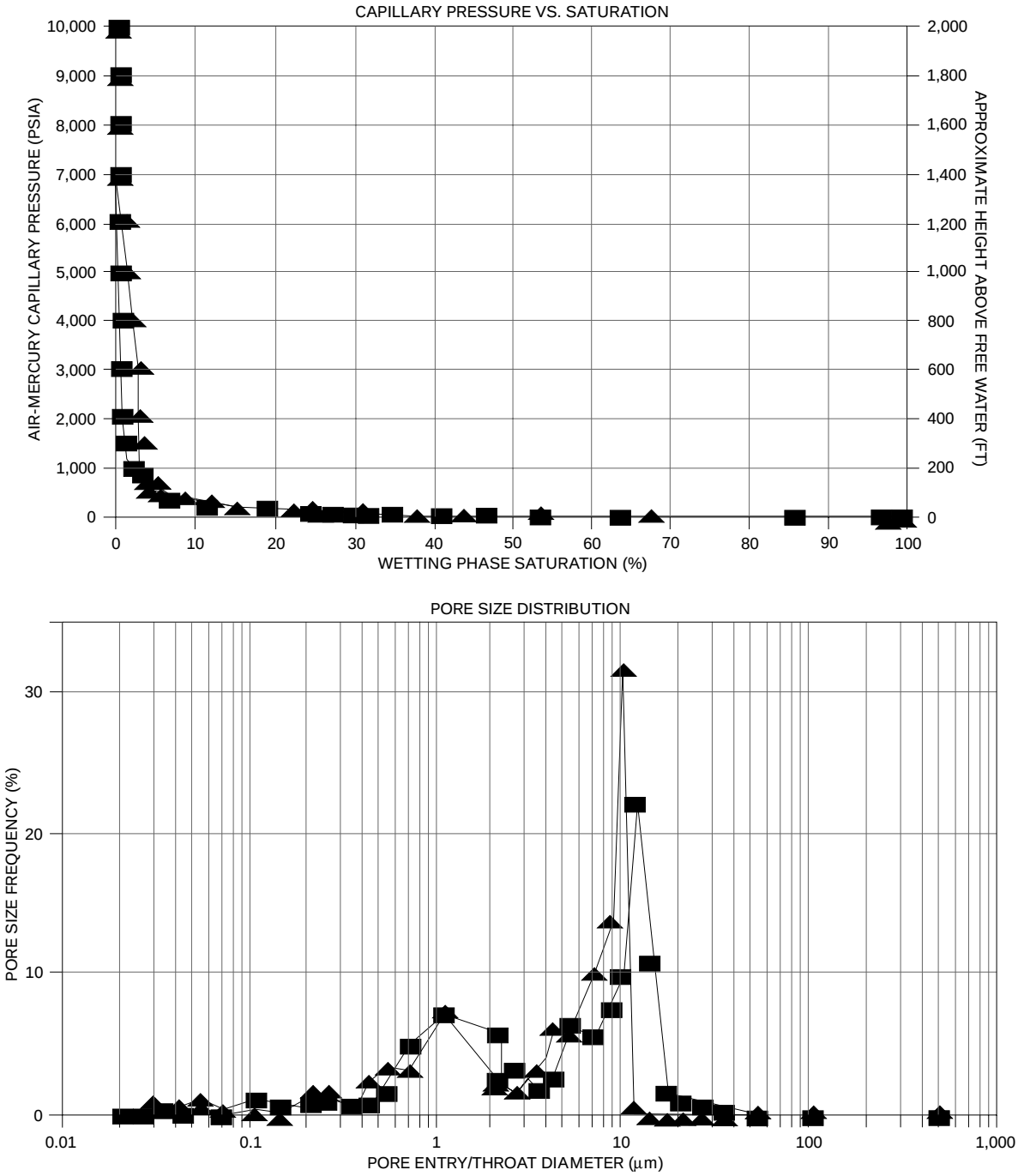

A

commonly much smaller, than the pores. These data also suggest that pore throats, rather than stress-relief microfractures, are indeed being closed by increased confining stress.

DISCUSSION

Pores and pore throats are initially controlled by depositional patterns and facies and are subsequently modified by diagenetic processes. It is usually possible to identify and trace depositional facies through the use of geophysical logs, although these data are commonly too widely spaced to adequately define facies distribution. It is not generally possible, however, because of wide variations in diagenetic processes, to predict capillary pressure characteristics, which are a measure of pore-throat characteristics, from knowledge of depositional lithofacies. It is necessary to generate the data for calculation of pore-throat characteristics from

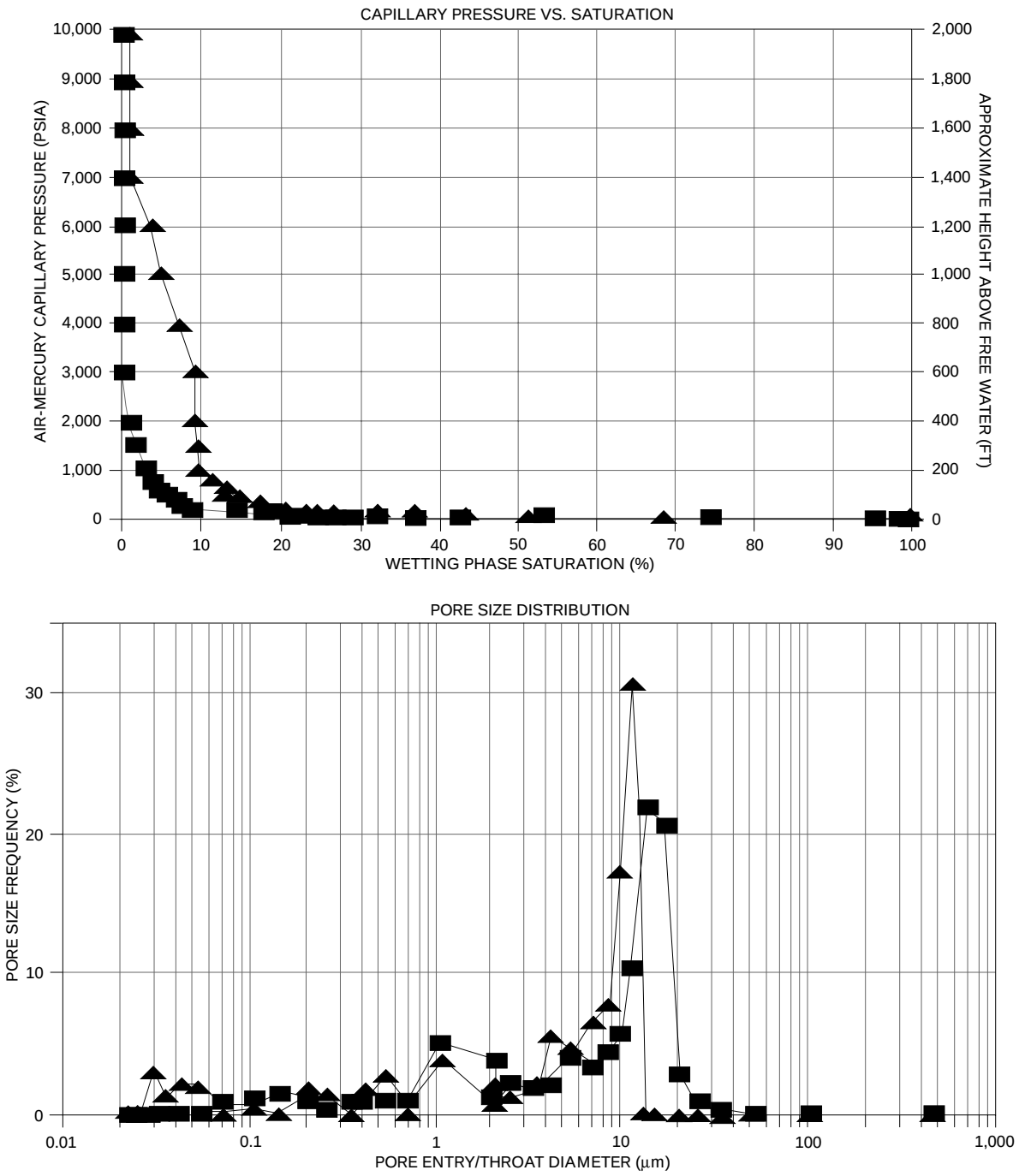

B

measurements on core samples; supporting data can be obtained from examination of thin sections and from scanning electron microscopy.

Data from this study show that pore throats, the controlling structure in the flow of fluids through a pore network, are typically smaller than pores in thin section or apparent in hand specimen. Pore throats, especially small (<0.1 μm) pore throats, common in fine-grained to very fine grained clastic rocks, are very sensitive to confining stress and probably act as limiting factors controlling flow of gas to a well bore. Small pore throats are also very sensitive to formation fluids, which reduce their effective diameter. Measurement of capillary pressure under confining stress suggests that, although microfractures are induced by removing core from reservoir conditions and are closed during restoration of confining stress, constriction of very small pore throats is the controlling mechanism affecting fluid flow at reservoir conditions in the samples examined. These data aid in defining reservoir properties under in situ conditions and are available for reservoir description and for use in simulation studies.

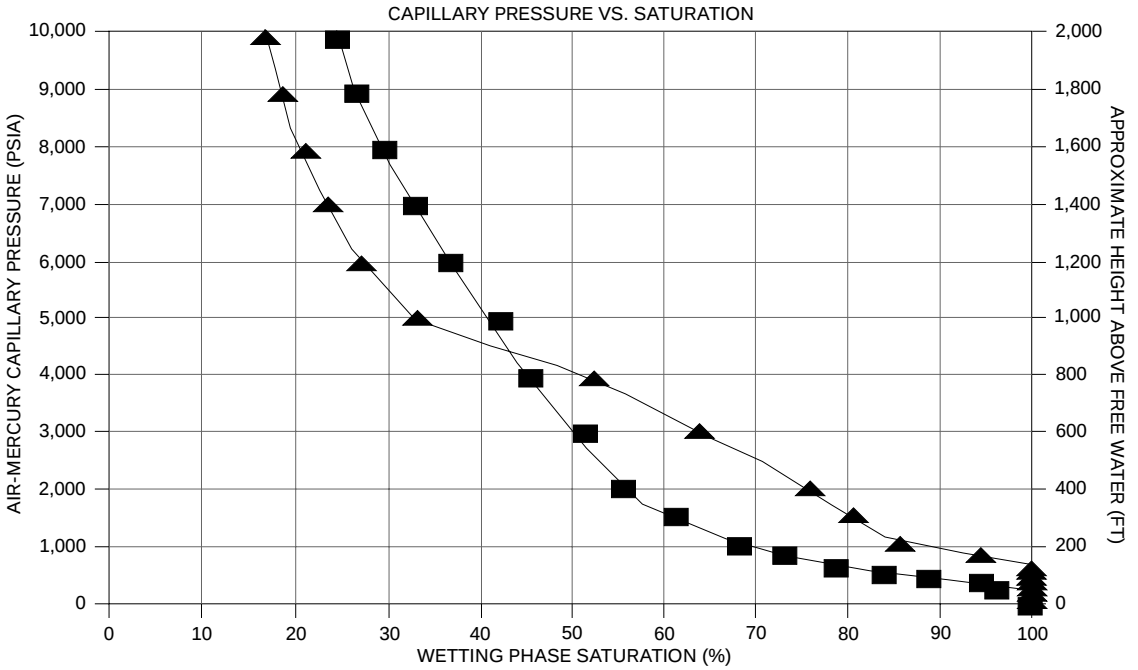

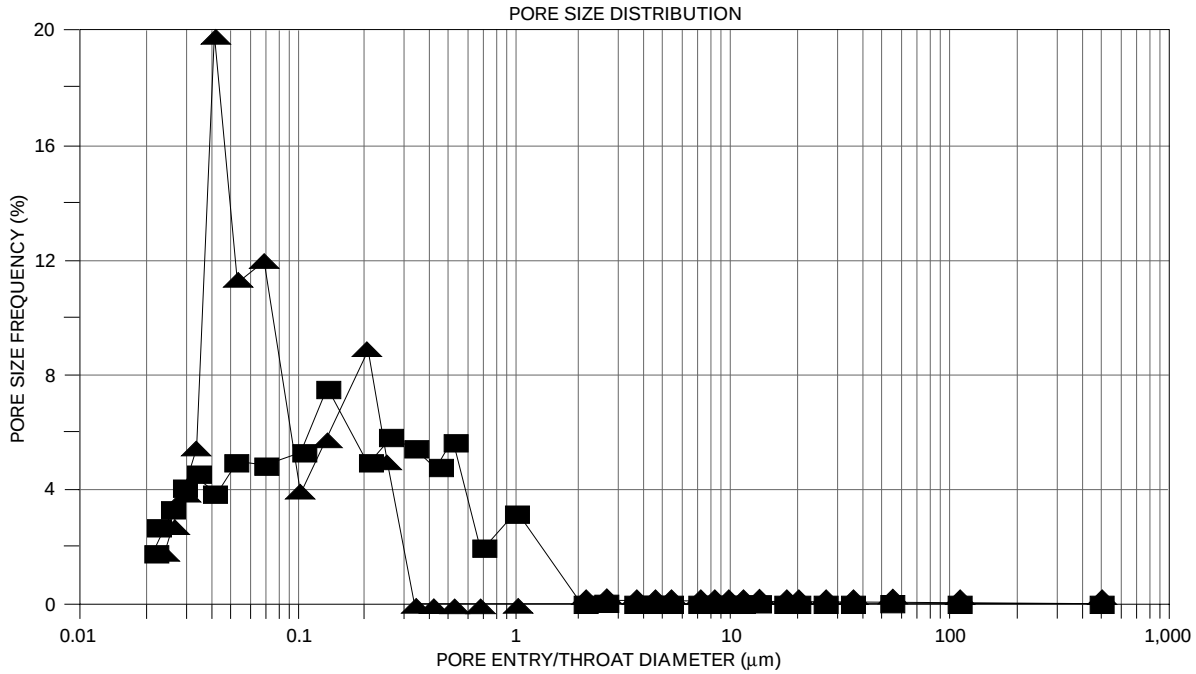

C

REFERENCES CITED

Atkins, J.E., and McBride, E. F., 1992, Porosity and packing of Holocene river, dune, and beach sands: American Association of Petroleum Geologists Bulletin, v. 76, no. 3, p. 339–355.

Bachu, S., and Underschulz, J. R., 1992, Regional-scale porosity and permeability variations, Peace River arch, Alberta: American Association of Petroleum Geologists Bulletin, v. 76, no. 4, p. 547–562.

Bloch, S., 1991, Empirical prediction of porosity and permeability in sandstones: American Association of Petroleum Geologists Bulletin, v. 75, no. 7, p. 1145–1160.

Dutton, S.P., and Diggs, T.N., 1992, Evolution of porosity and permeability in the Lower Cretaceous Travis Peak Formation, East Texas: American Association of Petroleum Geologists Bulletin, v. 76, no. 2, p. 252–269.

Harrison, W.J., 1989, Modeling fluid/rock interactions in sedimentary basins, *in* Cross, T.A., ed., Quantitative dynamic stratigraphy: New York, Prentice Hall, p. 195–231.

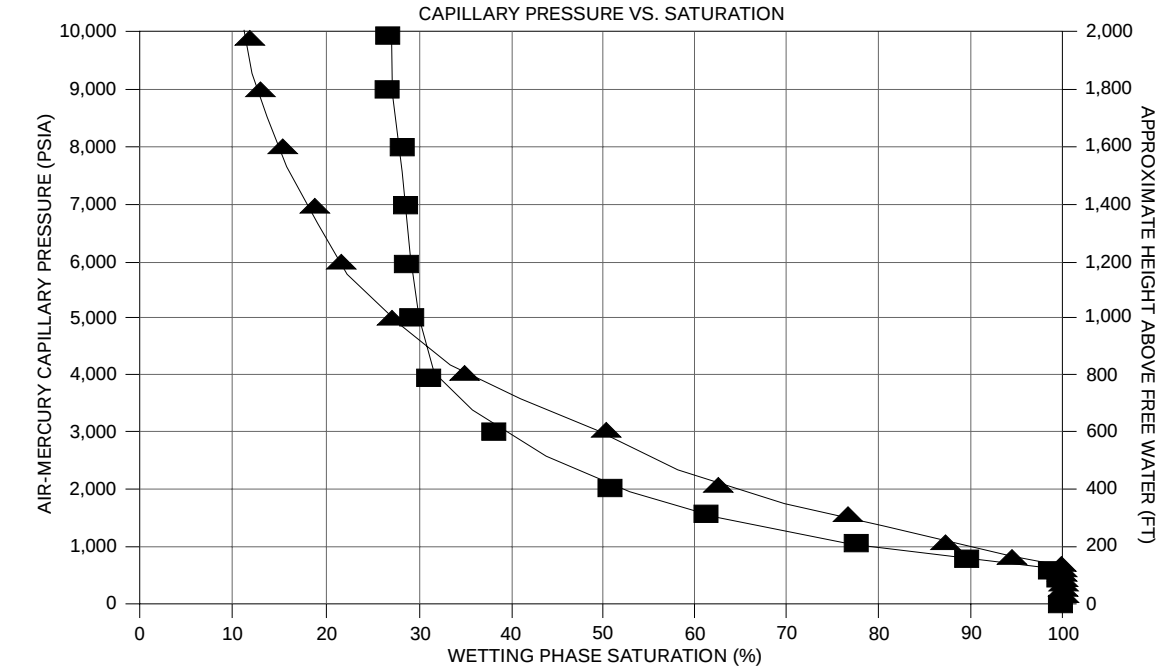

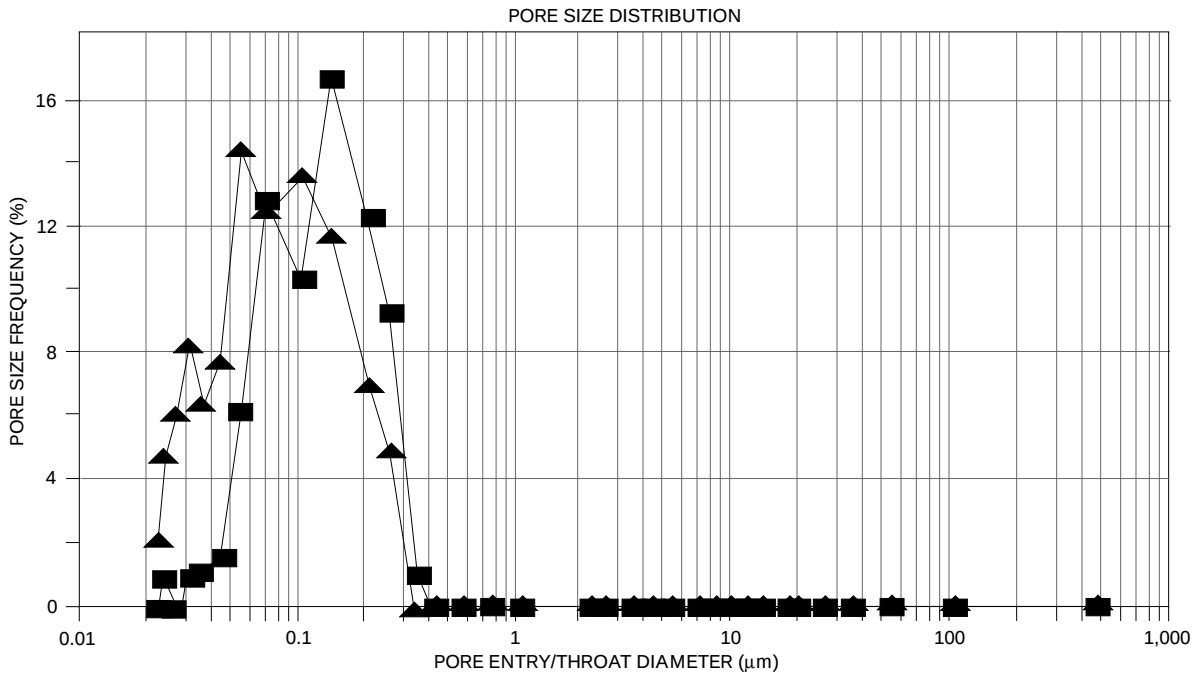

D

Keighin. C.W., and Flores, R.M., 1989, Depositional facies, petrofacies, and diagenesis of siliciclastics of Morrow and Springer rocks, Anadarko basin, Oklahoma: Oklahoma Geological Survey Bulletin 90, p. 147–161.

Klinkenberg, L.J., 1941, The permeability of porous media to liquids and gases, *in* Drilling and production practices: American Petroleum Institute, p. 200–213.

McBride, E.F., Diggs, T.N., and Wilson, J.C., 1991, Compaction of Wilcox and Carrizo sandstones (Paleocene-Eocene) to 4420 m, Texas Gulf Coast: Journal of Sedimentary Petrology, v. 61, no. 1, p. 73–85.

McCreesh, C.A., Ehrlich, R., and Crabtree, S.J., 1991, Petrography and reservoir physics II—Relating thin section porosity to capillary pressure, the association between pore types and throat size: American Association of Petroleum Geologists Bulletin, v. 75, no. 10, p. 1563–1578.

Purcell, W.R., 1949, Capillary-pressures—Their measurement using mercury and the calculation of permeability therefrom:

American Institute of Mining, Metallurgical, and Petroleum Engineers, Petroleum Transactions, v. 186, p. 39–48.

Sampath, K., and Keighin, C.W., 1982, Factors affecting slippage in tight sandstones of Cretaceous age in the Uinta Basin: Journal of Petroleum Technology, v. 34, no. 11, p. 2715–2720.

Schmoker, J.W., and Gautier, D.L., 1988, Sandstone porosity as a function of thermal maturity: Geology, v. 16, p. 1007–1010.

Surdam, R.S., Dunn, D.B., MacGowan, T.L., and Heasler, H.P., 1989, Conceptual models for the prediction of porosity evolution with an example from the Frontier Formation, Bighorn Basin, Wyoming, *in* Coalson, E.B., and others, eds., Petrogenesis and petrophysics of selected sandstone reservoirs of the Rocky Mountain region: Denver, Rocky Mountain Association of Geologists, p. 7–28.